

# Reply to “Comment on ‘Microwave vortex dissipation of superconducting Nd-Ce-Cu-O epitaxial films in high magnetic fields’ ”

N.-C. Yeh<sup>1</sup> and D. M. Strayer<sup>2</sup>

<sup>1</sup>*Department of Physics, California Institute of Technology, Pasadena, California 91125, USA*

<sup>2</sup>*Jet Propulsion Laboratory, California Institute of Technology, Pasadena, California 91107, USA*

(Received 6 December 2005; revised manuscript received 2 March 2006; published 16 August 2006)

We demonstrate with detailed analysis that the criticisms in the preceding Comment by Blackstead are largely due to insufficient understanding of the experimental issues associated with our system or the imposition of formalism that is inapplicable to our experiments. In particular, we distinguish the conventional formalism for “field-defined” surface resistance applicable to measurements on samples with filling factors (i.e., the ratio of the sample volume to that of the microwave cavity) approaching 1 from our “dissipation-defined” surface resistance derived from first principles for measurements on samples with very small filling factors.

DOI: [10.1103/PhysRevB.74.066502](https://doi.org/10.1103/PhysRevB.74.066502)

PACS number(s): 74.50.+r, 74.62.Dh, 74.72.-h

## I. INTRODUCTION

The Comment by Blackstead lists eight points of criticism on Refs. 1 and 2. We elaborate in this Reply that these criticisms are largely due to insufficient understanding of relevant experimental issues and the imposition of theoretical formalism that is inapplicable to the physical system considered in our paper.

The reply is structured as follows. Section II provides comprehensive descriptions for the experimental setup and calibration procedures, as well as the sensitivity and accuracy of the system. In Sec. II we provide the physical foundation that explains why the formalism given in the Comment leads to unphysical results in the thin film limit and is thus inapplicable to our experimental observation. In Sec. IV we address all issues in the Comment point by point.

## II. THE EXPERIMENTAL APPARATUS AND CALIBRATION PROCEDURES

We begin with specifying additional experimental details that could not be included in the original Ref. 1 and the Erratum in Ref. 2, although some related information was readily available in Ref. 3. These details are directly relevant to clarifying various misconceptions in the Comment. Our experimental apparatus for microwave measurements involves a sapphire-loaded copper cavity, as schematically illustrated in Fig. 1. The sapphire ring resonator supports various high- $Q$  whispering gallery (WG) modes, as exemplified in Figs. 2(a) and 2(b), and the  $Q$  values of these modes are insensitive to the application of external magnetic fields, because magnetic fields do not induce losses on pure sapphire, and the gold-plated copper walls of the cavity are far from the evanescent fields of the WG modes so that magnetic-field-induced excess dissipations on the cavity walls do not make significant contributions to the stored electromagnetic energies associated with the WG modes. The high- $Q$  nature ( $Q > 10^7$  at 4.2 K) of the sapphire-loaded copper cavity, its insensitivity to large magnetic fields, and the availability of many high- $Q$  modes were the primary reasons for us to employ such a system to study high-field vortex dissipation in type-II superconductors.<sup>1,4</sup>

Despite the aforementioned advantages of the sapphire-loaded microwave cavity, there are a number of shortcomings for using such an apparatus for material characterizations. First, in our experiments the sample being tested is placed directly under the driving coax to expose it to an antinode of the resonant mode pattern. Consequently, the WG mode patterns and the quality factor ( $Q$ ) of the modes are very sensitive to perturbations near the sapphire ring and therefore reveal significant dependence on the position and geometry of the sample to be characterized, as manifested in

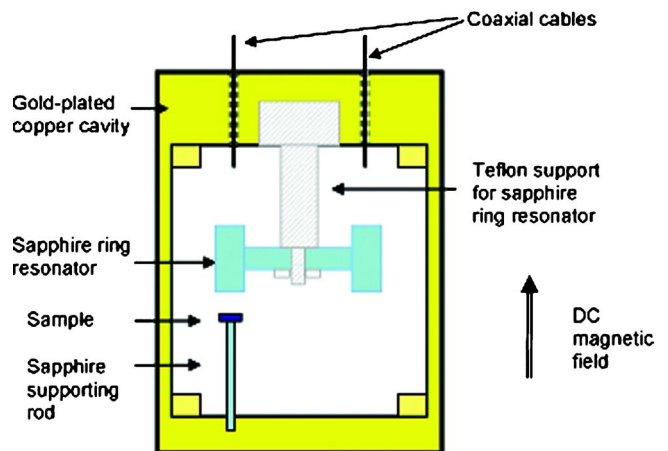


FIG. 1. (Color online) Schematics of the cross-sectional side view of our sapphire-loaded microwave cavity. The sapphire supporting rod for the sample was placed directly underneath an antinode of the WG modes. The distance between the tip of the sapphire rod and the sapphire ring must be sufficiently far to ensure weak perturbation to the WG mode patterns. Similarly, the sample placed on top of the sapphire rod must be sufficiently small in both its area and thickness to ensure minimum perturbation to the WG modes. On the other hand, the distance between the sample and the sapphire ring could not be too large in order to achieve detectable microwave losses. Evidently the filling factor of a sample in such a sapphire-loaded microwave cavity was very small ( $\approx 1\%$ ) compared with a typical microwave measurement apparatus. The small filling factor and the strong sensitivity to sample geometry were the primary reasons for limited accuracy in the measurements of surface resistance.

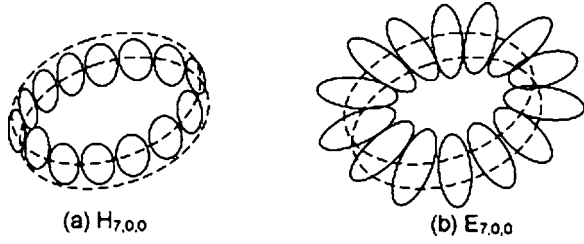


FIG. 2. Illustrations of the magnetic field distributions of whispering gallery modes supported by a sapphire ring resonator: (a)  $H_{7,0,0}$  and (b)  $E_{7,0,0}$  mode. Note that the electromagnetic fields of the modes are concentrated around the resonator, with slight extension outside the sapphire ring into the evanescent region.

Fig. 1. The small filling factor (i.e., a small volume ratio of the sample to the cavity) of our experimental configuration further amplifies the complication associated with the sensitive dependence on the WG mode pattern. These inherent limitations result in significant uncertainties in the accuracy of the measured surface resistance, despite the high sensitivity of the apparatus. That is, the absolute values of the surface resistance of samples cannot be very accurately determined with a single piece of bulk calibration material of known surface resistance, because the calibration material may not have exactly the same size, shape, and thickness as the sample to be measured, and variations in the position of the sapphire supporting rod (see Fig. 1) for the sample due to thermal cycling can also result in uncertainties in the measurement of microwave losses. These uncertainties were manifested by our measurements of the surface resistance of pure gold foils, and the uncertainties in the absolute value of the surface resistance were in the range 2–20 m $\Omega$ , depending on the temperature range of our measurements, the geometry of the calibration material, and the relative position between the sample and the sapphire ring oscillator. In addition, for different WG modes, the corresponding antinode positions relative to the sample vary, so that calibrations must be carried out individually for each WG mode, which leads to higher degrees of uncertainties in determining the frequency dependence of  $R_s$ . On the other hand, measurements on superconducting samples revealed that the apparatus had very high sensitivity despite limited accuracy. Specifically, for a given WG mode, the system could detect very small relative changes in the surface resistance of samples as a function of the temperature  $T$  and magnetic field  $H$ , because small changes in the total  $Q$  values of the microwave cavity loaded with samples of a small filling factor could be detected as  $T$  and  $H$  are varied. The sensitivity, when converted into surface resistance, was  $\sim 10 \mu\Omega$ , while the accuracy for measurements over a temperature range from 4.2 to  $\sim 30$  K was  $\sim 2$  m $\Omega$ . The sensitivity for our apparatus was reported in Ref. 1.

Given the limited accuracy in calibrations and our primary objective to investigate the relative changes of type-II superconducting thin films as a function of temperature and field in the superconducting state rather than the absolute values of the normal state surface resistance, we performed the following procedure to obtain the geometric factors for the microwave surface resistance of our samples. In the case

of measurements on bulk samples, the quality factor ( $Q_0$ ) of a microwave resonating mode ( $f_0$ ) in the absence of any sample was obtained through Lorentzian fitting to the microwave signal (in volts) vs frequency ( $f$ ) data near  $f_0$ .<sup>3</sup> Then the same measurement for a resonator loaded with a sample was performed, yielding a lower quality factor ( $Q_s$ ) and a slightly lower resonating frequency  $f_s$ . In the case of thin film samples on substrates, the background quality factor ( $Q_0$ ) of a microwave resonating mode ( $f_0$ ) was determined by measurements on a bare substrate with the same geometry as that of the thin-film-on-substrate sample. In general, the filling factor of our system was very small, on the order of  $\approx 1\%$  in the cavity, so that  $f_s$  did not deviate substantially from  $f_0$ . Hence, the total power loss ( $P_s$ ) associated with the sample, which was proportional to the surface resistance ( $R_s$ ) of the sample under a given electromagnetic (EM) field pattern of the resonator, could be obtained as follows:

$$P_s \propto 2\pi(f_s Q_s^{-1} - f_0 Q_0^{-1}) = \omega_s Q_s^{-1} - \omega_0 Q_0^{-1} \approx \omega_0(Q_s^{-1} - Q_0^{-1}) \equiv c_s R_s. \quad (1)$$

In Eq. (1)  $c_s$  is a frequency-dependent calibration factor of the apparatus and  $R_s$  is the surface resistance of the sample empirically defined from  $\omega_0(Q_s^{-1} - Q_0^{-1}) \equiv c_s R_s$ , which is a function of frequency  $\omega$ ,  $T$ , and  $H$ . As stated previously, the experimentally measurable quantity was  $c_s R_s$  rather than  $R_s$ . Thus, calibrations against material with a known surface resistance at a fixed temperature were necessary to determine  $c_s$ . For a thin film superconductor of thickness  $d$  and a small filling factor in a microwave cavity under the EM fields of a WG mode, the theoretical value of the sample surface resistance in the normal state (see Sec. III for more details) is approximately  $R_s \sim \mu_0 \omega_0 d \propto \omega_0$ , whereas that of a bulk superconductor would be  $R_s \sim \mu_0 \omega_0 \delta_n \propto \omega_0^{1/2}$ , with  $\delta_n$  being the normal-state skin depth and  $\delta_n \propto \omega_0^{-1/2}$ . Thus,  $c_s$  could be obtained by measuring  $\omega_0(Q_s^{-1} - Q_0^{-1})$  above the superconducting transition  $T_c$  via the relation  $c_s \approx \omega_0(Q_s^{-1} - Q_0^{-1}) / (\mu_0 \omega_0 d)$ . The procedure for deducing microwave surface resistance of a sample from the measured microwave losses through calibration of the geometric factor against a known surface resistance is standard and was also described in Ref. 3. We further note that the  $T$  and  $H$  dependence of the surface resistance was independent of the calibrated geometric factor  $c_s$ , regardless of the accuracy in the absolute value of  $c_s$ . Hence, our procedure of using the normal-state surface resistance ( $\sim \mu_0 \omega_0 d$ ) of the film for calibrating the geometric factor could ensure best accuracy for the relative changes in the surface resistance of the superconducting sample under varying  $T$  and  $H$ . On the other hand, changes in  $R_s$  due to varying  $\omega$  for given  $T$  and  $H$  are less reliable because the WG mode patterns and thus the calibrations (including  $c_s$ ) are sensitive functions of  $\omega$ .

### III. MICROWAVE SURFACE RESISTANCES OF THIN FILMS WITH SMALL FILLING FACTORS

The major discrepancy between our results and the assertion in the Comment can be attributed to the imposition of an inapplicable formalism in the Comment on our experimental

data. Specifically, the underlying assumption that leads to the expression of the surface resistance in the Comment begins with the definitions of the surface impedance  $Z_s = E_{\parallel}/H_{\parallel}$  and surface resistance  $R_s = \text{Re}[Z_s]$ , where  $E_{\parallel}$  and  $H_{\parallel}$  are the tangential electric and magnetic field components relative to the surface of the sample. By further assuming a freely suspended slab of conducting sample and allowing propagation of the EM fields through the sample so that the electromagnetic fields recover full strength on both sides of the slab, one recovers the expression of surface resistance<sup>6</sup> given in the Comment.

The problem with this approach is that the definition for the surface resistance using  $E_{\parallel}$  and  $H_{\parallel}$  is representative of the energy dissipation on the sample only if the incident electromagnetic field energy in the volume of our consideration is entirely dissipated in the sample. This point can be understood by going back to the exact relation [Eq. (6.134) of Ref. 5] between the dissipated power in a sample and the Poynting vector  $\vec{S}$ :

$$\frac{1}{2} \int_{\text{vol}} (\vec{J}^* \cdot \vec{E}) d^3r + 2i\omega \int_{\text{vol}} (w_e - w_m) d^3r + \int_{\text{surf}} (\vec{S} \cdot \hat{n}) d^2r = 0, \quad (2)$$

where  $w_e$  and  $w_m$  denote the electric and magnetic field energy densities, and  $\hat{n}$  is the normal vector of the surface. From Eq. (2) it is clear that the definition of  $R_s \equiv \text{Re}[E_{\parallel}/H_{\parallel}]$  is proportional to the energy dissipation  $\int d^3r (\vec{J}^* \cdot \vec{E})/2$  only if the second term vanishes, implying that all electromagnetic energies in the volume of our consideration are dissipated in the sample. This approximation is therefore a good one if we consider measurements on samples of filling factors approaching 1 in a microwave cavity because the total volume under consideration equals that of the sample. On the other hand, the same definition would lead to serious overestimate of the real dissipation on a sample and is therefore invalid if the second term is substantial, such as in the case of microwave measurements on samples with very small filling factors. In other words, for a small sample filling factor inside a microwave cavity, the energy transmitted to the sample as determined by the Poynting vector is not equal to the energy dissipated in the sample because a large fraction of the energy transmitted will subsequently escape from the sample into the free space inside the microwave cavity. This situation is particularly acute for a thin film of a thickness much smaller than the microwave wavelength so that no standing waves can form within the film. (In our system the microwave wavelength is more than  $10^5$  times longer than our thin film thickness.) Hence, the field-defined surface resistance  $R_s \equiv \text{Re}[E_{\parallel}/H_{\parallel}]$  based on assuming complete dissipation of incident energy onto the sample [see Eq. (2)] does not represent the actual energy dissipated in the sample if the sample filling factor is small. In fact, a similar notion has also been pointed out by numerous authors<sup>7-12</sup> who investigated the surface resistance of conducting materials with relatively small sample filling factors in a variety of experimental apparatus. In those studies,<sup>7-12</sup> detailed theoretical analysis from first principles

rather than the definition of  $R_s \equiv \text{Re}[E_{\parallel}/H_{\parallel}]$  has been employed to analyze the dissipation-defined surface resistance.

In the following we consider a simple example that illustrates why the field-defined expression  $R_s \equiv \text{Re}[E_{\parallel}/H_{\parallel}]$  is generally not equivalent to the real dissipation in a conducting sample unless the sample thickness  $d$  is much larger than the skin depth  $\delta_n$ ; the latter corresponds to an effective sample filling factor approaching 1 because electromagnetic waves incident from one side of the sample can hardly escape from the other side. Specifically, we consider a free-standing metallic thin film of thickness  $d$  (along the  $\hat{z}$  axis) and resistivity  $\rho_n$  ( $\equiv \sigma_n^{-1}$ ), and assume that microwaves are incident from vacuum in region 1 ( $z < 0$ ) onto the conducting sample in region 2 ( $0 \leq z \leq d$ ), and the backside of the sample in region 3 ( $z > 0$ ) is a uniform dielectric medium such as vacuum with the field-defined surface impedance being  $Z_0^{(3)} = Z_{s,\text{vac}} = R_{s,\text{vac}} = (\mu_0/\epsilon_0)^{1/2} = 376.7 \Omega$ . Assuming plane waves for the incident electromagnetic fields, we solve Maxwell's equation and Ohm's law with proper boundary conditions at  $z=0$  and  $z=d$  for both forward- and backward-moving waves. We therefore obtain a general expression for the surface impedance of the conducting sample at  $z=0$ :

$$Z_s = Z_0^{(2)} \frac{1 + F^{(2)}}{1 - F^{(2)}}, \quad F^{(2)} \equiv e^{-2ik_z^{(2+)d}} \frac{Z_0^{(3)} - Z_0^{(2)}}{Z_0^{(3)} + Z_0^{(2)}}, \quad (3)$$

where  $k_z^{(2+)}$  refers to the  $z$  component of the wave vector of the forward-traveling waves in region 2, and the impedances  $Z_0^{(M)}$  for  $M=1,2,3$  depend on the polarization and are given by

$$Z_0^{(M)} = \frac{\mu_0 \omega}{k_z^{(M)}} \text{ for } \vec{E} = E_0 \hat{y} \quad (4)$$

$$Z_0^{(M)} = \frac{\mu_0 \omega k_z^{(M)}}{k^2} \text{ for } \vec{H} = H_0 \hat{y}, \quad (5)$$

and the wave vector is defined as  $\vec{k} = k_x \hat{x} + k_z \hat{z}$ . Specifically,  $(k^{(2+)})^2 = \epsilon_r (\omega/c)^2 - i\mu_0 \omega \sigma_n = \epsilon_r (\omega/c)^2 - i(2/\delta_n^2)$ , where  $\epsilon_r$  is the relative dielectric constant of the conducting sample. Equation (3) clearly shows that for a general thickness  $d$ , the surface impedance of the conducting samples depends on properties of regions 2 and 3 but not on region 1.

Given Eq. (3), we now consider two extreme cases. First, in the bulk limit  $d \gg \delta_n$ , we have  $F^{(2)} \rightarrow 0$  so that  $Z_s \rightarrow Z_0^{(2)}$ , implying that  $Z_s$  becomes solely dependent on the properties of the conducting sample in region 2. Furthermore, for nearly normal incident waves, we have  $Z_0^{(2)} = \mu_0 \omega / k_z^{(2+)}$  for both polarizations, and  $(k_z^{(2+)})^2 \approx k^2 \approx -i(2/\delta_n^2)$  so that

$$Z_s(d \gg \delta_n) \approx Z_0^{(2+)} \approx \frac{(1+i)}{\sqrt{2}} \mu_0 \omega \delta_n = (\mu_0 \omega \rho_n)^{1/2} (1+i), \quad (6)$$

which recovers the well-known result for bulk surface impedance of a conducting material. On the other hand, we have from Eq. (3)

$$Z_s = Z_0^{(2)} \frac{Z_0^{(3)} \cos(k_z^{(2+)} d) + i Z_0^{(2)} \sin(k_z^{(2+)} d)}{Z_0^{(2)} \cos(k_z^{(2+)} d) + i Z_0^{(3)} \sin(k_z^{(2+)} d)} \quad (7)$$

so that in the thin film limit where  $d \ll \delta_n$  and  $k_z^{(2)} d \ll 1$ ,

$$\begin{aligned} Z_s(d \ll \delta_n) &\approx \left( \frac{\mu_0 \omega}{k_z^{(2+)}} \right) \frac{Z_0^{(3)} + i(\mu_0 \omega d)}{i Z_0^{(3)} k_z^{(2+)} d + [\mu_0 \omega / k_z^{(2+)}]} \\ &\approx \{i[(k_z^{(2+)})^2 d / (\mu_0 \omega)] + [1/Z_0^{(3)}]\}^{-1} \\ &\approx \{[2d / (\mu_0 \omega \delta_n^2)] + [1/Z_0^{(3)}]\}^{-1} \\ &\approx [(d/\rho_n) + (1/Z_0^{(3)})]^{-1}. \end{aligned} \quad (8)$$

Consequently,  $Z_s \rightarrow Z_0^{(3)} = Z_{s,vac}$  for  $d \rightarrow 0$  from Eq. (8), which is reasonable because vacuum impedance must be recovered in the absence of a conducting sample in region 2. It is also noteworthy that the recovery of vacuum impedance and therefore a finite  $R_{s,vac}$  is by no means indicative of any dissipation in vacuum, which confirms our earlier statement that the field-defined dissipation for a small sample filling factor cannot be equivalent to the true dissipation in the sample.

Our findings given in the above example are fundamentally different from the expression  $R_s = \rho_n / d$  given in the Comment; the latter yields  $R_s \rightarrow \infty$  for  $d \rightarrow 0$ , implying an unphysical result of infinite dissipation in vacuum if one were to equate the field-defined surface resistance to the dissipation-defined surface resistance. The unphysical result in the Comment is because it does not account for the contribution from region 3 in the thin sample limit and it assumes that the Poynting theory is applicable to a situation of a very small sample filling factor. Thus, the field-defined surface resistance given in the Comment leads to a severe overestimate of actual energy dissipation in a free-standing thin film sample. It is therefore not meaningful to compare the formalism given in the Comment with the real microwave dissipation determined in our experiments.

Having shown that the field-defined surface resistance cannot account for true sample dissipation in the thin-film limit, we return to the first-principles derivation for microwave dissipation in Ref. 1. The derivation started with calculating the power dissipation ( $P_{tot}$ ) on the sample due to an induced current density ( $J$ ) inside the sample under incident electromagnetic waves. Unlike the field-defined surface resistance based on the applicability of the Poynting theorem, the first-principles derivation does not assume the condition of complete energy transmission to the sample, and is therefore a much better approach to estimating the microwave dissipation for a small sample filling factor, provided that proper boundary conditions are considered.<sup>8-10</sup> Moreover, the first-principles calculation in Ref. 1 recovers the field-defined definition of the microwave surface resistance if the sample filling factor approaches 1, and in the limit of  $d \rightarrow 0$  it also yields the correct result of zero dissipation. Specifically, our first-principles derivation for the surface resistance in Ref. 1 led to an expression for  $R_s$  in terms of the power dissipation  $P_s$  and a calibration coefficient consisting of the geometric factor and the microwave power:

$$P_{tot} = \text{Re} \left[ \frac{1}{2} \int_{\text{vol}} \vec{J}^* \cdot \vec{E} d^3 r \right] \equiv (A h_0^2) R_s. \quad (9)$$

Here the integration is over the effective sample volume,  $A$  is the effective surface area of the sample,  $E$  denotes the electric field component, and  $h_0$  is the amplitude of the incident magnetic field. Hereafter we refer to the surface resistance defined by Eq. (9) as the “dissipation-defined” surface resistance so as to distinguish it from the “field-defined” surface resistance  $R_s = \text{Re}[E_{\parallel}/H_{\parallel}]$ . As discussed earlier, there are differences between the field-defined and dissipation-defined surface resistances of a sample, and it can be easily shown that these two definitions become equivalent to each other if the filling factor of a sample approaches 1, corresponding to complete transmission of the incident electromagnetic energy to the sample according to the Poynting theorem.<sup>5</sup> Given that our experiments involved thin-film samples of very small filling factors and that our experiments measured dissipation rather than the local electromagnetic fields on the surface of the sample, it is only meaningful to compare the dissipation-defined rather than the field-defined surface resistance with our experimental data.

To proceed with the derivation, we need to find the correct spatial dependence of the induced current density and electromagnetic fields in the thin-film sample. This task involves finding the solutions to the magnetic field  $h(z) \parallel \hat{x}$  (a polarization consistent with our experimental configuration) as a function of  $z$ , where  $z$  is from now on defined as the distance measured from the center of a platelike sample. In Ref. 1 we assumed an exponentially decaying functional form for the evanescent magnetic field, which was the lowest-order approximation. We consider in the following a more general case with additional boundary conditions imposed, and we demonstrate that the resulting field-defined surface resistance still recovers the finding given in Ref. 1 in the lowest-order approximation.

We begin with a formula suitable for intermediate-thickness superconducting films with proper boundary conditions to derive the total dissipation for a free-standing superconducting sample with a thickness  $d$  that is much smaller than the wavelength of the incident microwaves ( $2\pi c/\omega$ ) but otherwise can be either larger or smaller than the effective penetration depth  $|\lambda_{\text{eff}}|$  (which is a nonlocal penetration depth derived in Refs. 13 and 14 and reduces to  $\delta_n/\sqrt{2}$  for  $T > T_c$  in the normal state). Here  $c$  denotes the speed of light and  $\omega$  is the angular frequency of the incident wave. We note that the free-standing platelike approximation for calculating the dissipation is reasonable because of the small sample filling factor in our experiments and also because the substrate contribution has been subtracted out in the calibration procedure. For a free-standing platelike superconducting sample of thickness  $d \ll (2\pi c/\omega_0)$  under a transverse magnetic field, the magnetic field at two surfaces of the sample may be approximated as  $\vec{h}(z = \pm d/2, t) = h_0 e^{-i\omega t} \hat{x}$ . This approximation is applicable to microwave measurements on most samples because the wavelength is on the order of centimeters for microwave frequencies of  $\sim 10^{10}$  Hz. Thus, the magnetic field  $\vec{h}(z, t)$ , electric field  $\vec{E}(z, t)$ , and induced cur-

rent density  $\vec{J}(z, t)$  inside the sample for  $-d/2 \leq z \leq d/2$  can be approximated by the following:

$$\begin{aligned}\vec{h}(z, t) &= h_0 e^{-i\omega t} \frac{\cosh(z/\lambda_{\text{eff}})}{\cosh(d/2\lambda_{\text{eff}})} \hat{x}, \\ \vec{E}(z, t) &= i\mu_0\omega h_0 \lambda_{\text{eff}} e^{-i\omega t} \frac{\sinh(z/\lambda_{\text{eff}})}{\cosh(d/2\lambda_{\text{eff}})} \hat{y}, \\ \vec{J}(z, t) &= i \frac{h_0 e^{-i\omega t}}{\lambda_{\text{eff}}} \frac{\sinh(z/\lambda_{\text{eff}})}{\cosh(d/2\lambda_{\text{eff}})} \hat{y}.\end{aligned}\quad (10)$$

Noting that  $\lambda_{\text{eff}}$  is complex for time-dependent electromagnetic fields and  $\lambda_{\text{eff}} = \lambda_R + i\lambda_I$ , where  $\lambda_R$  and  $\lambda_I$  represent the real and imaginary parts of the penetration depths, respectively, we calculate the total power dissipation inside the free-standing superconducting film and find that

$$\begin{aligned}P_{\text{tot}} &= \frac{1}{2} \text{Re} \left[ \int_{\text{vol}} \vec{J}^* \cdot \vec{E} d^3r \right] \\ &= \mu_0\omega A h_0^2 \left[ \frac{\lambda_I \sinh(d\lambda_R/|\lambda_{\text{eff}}|^2) - \lambda_R \sin(d\lambda_I/|\lambda_{\text{eff}}|^2)}{\cosh(d\lambda_R/|\lambda_{\text{eff}}|^2) + \cos(d\lambda_I/|\lambda_{\text{eff}}|^2)} \right].\end{aligned}\quad (11)$$

Thus, the corresponding dissipation-defined surface resistance is

$$\begin{aligned}R_s &= P_{\text{tot}}/(Ah_0^2) \\ &= \mu_0\omega \left[ \frac{\lambda_I \sinh(d\lambda_R/|\lambda_{\text{eff}}|^2) - \lambda_R \sin(d\lambda_I/|\lambda_{\text{eff}}|^2)}{\cosh(d\lambda_R/|\lambda_{\text{eff}}|^2) + \cos(d\lambda_I/|\lambda_{\text{eff}}|^2)} \right].\end{aligned}\quad (12)$$

For  $T > T_c$  and  $H=0$ ,  $\lambda_R = \lambda_I = \delta_n/2 \equiv \sqrt{\rho_n/(2\mu_0\omega)}$  if  $d > \delta_n/\sqrt{2}$ , so that the dissipation-defined  $R_s$  becomes

$$\begin{aligned}R_s(T > T_c) &\rightarrow \frac{\mu_0\omega\delta_n}{2} \left[ \frac{\sinh(d/\delta_n) - \sin(d/\delta_n)}{\cosh(d/\delta_n) + \cos(d/\delta_n)} \right] \\ &= \frac{\rho_n}{\delta_n} \left[ \frac{\sinh(d/\delta_n) - \sin(d/\delta_n)}{\cosh(d/\delta_n) + \cos(d/\delta_n)} \right].\end{aligned}\quad (13)$$

This dissipation-defined normal-metal surface resistance in Eq. (13) differs from the field-defined normal-metal surface resistance given in Ref. 6 and the Comment except in the thick-film ( $d \gg \delta_n$ ) limit. Here the field-defined formula<sup>6</sup> is explicitly given by

$$R_{s,\text{field}}(T > T_c) = \frac{\rho_n}{\delta_n} \left[ \frac{\sinh(2d/\delta_n) + \sin(2d/\delta_n)}{\cosh(2d/\delta_n) - \cos(2d/\delta_n)} \right].\quad (14)$$

As discussed previously, the field-defined  $R_s$  given in Eq. (14) tends to overestimate the energy dissipated in the sample unless the electromagnetic field energies within the volume of consideration are mostly transmitted to the sample, such as in the case of a sample filling factor approaching 1 or for a bulk sample with sample dimensions  $\gg \delta_n$ . Consequently, the dissipation-defined  $R_s$  in Eq. (13) and the field-defined  $R_s$  in Eq. (14) become identical in the bulk limit ( $d \gg \delta_n$ ) as expected from Poynting's theorem, and

$R_s(T > T_c) \rightarrow (\rho_n/\delta_n) = (\mu_0\omega\rho_n/2)^{1/2}$ , which is a well-known result. On the other hand, we stress that the expression in Eq. (14) overestimates the effective energy losses of a free-standing thin-film sample and leads to the unphysical limit  $R_s \rightarrow \infty$  for  $d \rightarrow 0$ . Therefore, it is the dissipation-defined  $R_s$  in Eq. (13) rather than the field-defined  $R_s$  in Eq. (14) that provides adequate comparison with our empirically determined microwave losses.

Next, we consider the dissipation-defined surface resistance in the thin-film limit where  $d < |\lambda_{\text{eff}}|$ . From Eq. (13) we obtain

$$R_s(T, H, \omega) \approx \left( \frac{\mu_0\omega}{6} \right) \frac{d^3 \lambda_R \lambda_I}{|\lambda_{\text{eff}}|^4}.\quad (15)$$

Assuming the Coffey-Clem nonlocal model,<sup>13,14</sup> we find that for  $T > T_c$  and  $H=0$ ,  $\lambda_R = \lambda_I = |\lambda_{\text{eff}}|/\sqrt{2} = \delta_n/2$  if  $d > \delta_n/2$ , whereas  $\lambda_R \approx \lambda_I \rightarrow d$  if  $d < \delta_n/2$ . Hence,  $R_s$  becomes

$$R_s(T > T_c) \rightarrow \begin{cases} \left( \frac{\mu_0\omega\delta_n^2}{24d} \right) & \text{if } \frac{\delta_n}{2} < d < \frac{\delta_n}{\sqrt{2}}, \\ \left( \frac{\mu_0\omega d}{6} \right) & \text{if } d < \frac{\delta_n}{2}, \end{cases}\quad (16)$$

Thus, the dissipation-defined normal-state surface resistance of a free-standing film with proper boundary conditions also vanishes for  $d \rightarrow 0$  according to Eq. (16), which is consistent with, although smaller than, the result given in our paper<sup>1</sup> for one-sided incident microwaves. The reason why the total dissipation in the free-standing thin film is smaller than that obtained from only forward-traveling waves is that the reflected waves reduce the total field strength inside the sample, thus resulting in smaller dissipation.

It is worth noting that from Eqs. (12), (13), (15), and (16), the expression of dissipation-defined  $R_s$  is generally dependent on the material properties (such as  $\delta_n$ ,  $\lambda_R$ , and  $\lambda_I$ ) of the sample for most sample thicknesses except in the extremely thin-film limit when  $d < \delta_n/2$ , where the dissipation of the sample becomes only dependent on the sample thickness  $d$  and the microwave frequency. This finding is sensible because in the extremely thin-film limit there is incomplete screening of the electromagnetic fields in the sample. That is, there is incomplete development of the skin depth  $\delta_n = (2\rho_n/\mu_0\omega)^{1/2}$  such that only the geometric effect (i.e., the thickness  $d$ ) rather than the sample characteristics (i.e., the resistivity  $\rho_n$ ) is realized.

#### IV. POINT-BY-POINT REPLY TO THE CRITICISMS

(1) Having given the calibration procedure described in Sec. II (which was also described in the published Erratum<sup>2</sup> although in less detail), we have effectively answered point 1 in the Comment regarding the alleged ‘‘unknown scaling’’ to our data in the Erratum.<sup>2</sup> Specifically, we have shown in Sec. II that the total power loss ( $P_s$ ) associated with the sample is proportional to the surface resistance ( $R_s$ ) of the sample via Eq. (1):  $P_s \propto c_s R_s \equiv \omega_0(Q_s^{-1} - Q_0^{-1})$ , where  $c_s$  is a frequency-dependent calibration factor of the apparatus and  $R_s$  is the dissipation-defined surface resistance of the sample, which is

a function of  $\omega$ ,  $T$ , and  $H$ . The quantity measurable in our experiments is  $c_s R_s \equiv \omega_0(Q_s^{-1} - Q_0^{-1})$  rather than  $R_s$ . Thus, calibrations against material with a known surface resistance at a fixed  $T$  are necessary to determine  $c_s$ . We have also shown in Sec. III that for a thin-film superconductor of thickness  $d$  and a very small filling factor in a microwave cavity, the dissipation-defined surface resistance of the sample in the normal state is  $R_s \sim \mu_0 \omega_0 d \propto \omega_0$ , whereas that of a bulk superconductor would be  $R_s \sim (\rho_n / \delta_n) = (\mu_0 \omega_0 \rho_n / 2)^{1/2} \propto \omega_0^{1/2}$ . Thus,  $c_s$  can be obtained by measuring  $P_s$  above the superconducting transition  $T_c$  via the relation  $c_s \sim P_s / (\mu_0 \omega_0 d)$ . This conversion step was the place where mistakes were made in our original paper.<sup>1</sup> That is, rather than taking the thin-film limit with  $R_s \sim \omega_0$ , one of us mistakenly used the bulk formula  $R_s \sim \omega_0^{1/2}$  and thus a wrong calibration factor  $c'_s$ . Hence, for two different resonating modes at  $\omega_1$  and  $\omega_2$ , we had a simple relation between the correct and the wrong calibration factors:

$$[c_s(\omega_1)/c'_s(\omega_1)]/[c_s(\omega_2)/c'_s(\omega_2)] = (\omega_2/\omega_1)^{1/2}. \quad (17)$$

In our experiment,  $\omega_1 = 2\pi \times (12.34 \text{ GHz})$  and  $\omega_2 = 2\pi \times (18.289 \text{ GHz})$ . Therefore the rescaling factor ( $c_s/c'_s$ ) has a ratio of  $(18.289/12.34)^{1/2} \approx 1.2$ , which is exactly what we had shown in the Erratum for the data. As for the theoretical fitting curves, our fitting program employed the expression  $R_s(T, H, \omega) \equiv R_s(T > T_c, \omega) F(T, H, \omega)$ , where the function  $F(T, H, \omega)$  varied from 0 and 1, with  $F(T, H, \omega) \rightarrow 1$  for  $T \rightarrow T_c$ . Thus, when we reported the correction in our Erratum,<sup>2</sup> we simply replaced the wrong input value in the program for  $R_s(T > T_c, \omega)$  by the correct value  $(\mu_0 \omega_0 d)$ , and the resulting theoretical curves scaled accordingly. Hence, the scaling of all curves and data points was well accounted for, as described in the Erratum.<sup>2</sup>

Additionally, as detailed in Sec. II, the accuracy of our surface resistance measurement was  $\sim 2 \text{ m}\Omega$  for temperatures between 4.2 and  $\sim 30 \text{ K}$ . Taking into consideration the experimental uncertainties of  $\sim 2 \text{ m}\Omega$  in the absolute (but not relative) value of the surface resistance, we find that the curves in Fig. 1 of the Comment are in fact consistent with what we gave in Ref. 2 within our specified experimental errors.

Regarding the reason why the data on Y-Ba-Cu-O film were not rescaled in the same way as in the case of the Nd-Ce-Cu-O film, it was because the calibration of Y-Ba-Cu-O was done correctly without the same mistake as that in the calibration of the Nd-Ce-Cu-O film.

(2) The Comment criticizes “whole numbers, with no decimal fractions” in the fitting parameters given in our paper. This criticism is apparently due to misinterpretation of our expression of the numbers. The numbers were expressed in whole numbers because of limited significant digits. For instance, “ $k_p(0) = 460 \text{ N T}^{1/2}/\text{m}^2$  for  $f = 18.289 \text{ GHz}$ ” means that  $k_p(0)$  only has two significant digits, and therefore the corresponding uncertainty is  $\pm 10 \text{ N T}^{1/2}/\text{m}^2$ .

(3) The Comment criticizes the result of our surface resistance in the thin-film limit by raising various issues, including recent findings in Ref. 15 of larger  $R_s$  values in Pr-Ce-Cu-O single crystals at 1.2 K than the normal-state  $R_s$

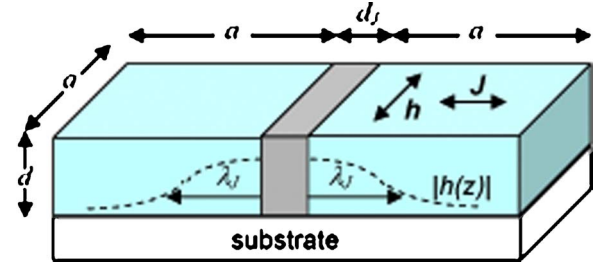


FIG. 3. (Color online) An effective circuit model by Hylton *et al.* (Ref. 16). The notations are defined in the text.

value of the Nd-Ce-Cu-O thin-film sample reported by us, and the absence of material dependence of the normal-state  $R_s$ . These criticisms are answered by our discussions in Sec. III. Specifically, we note that the dissipation-defined surface resistance does depend on material parameters except in the extremely thin-film limit (with  $d < \rho_n/2$ ), as shown in Eqs. (12), (13), (15), and (16) in Sec. III. For a bulk sample at  $T \rightarrow 0$ , our dissipation-defined surface resistance yields  $R_s \rightarrow \mu_0 \omega \lambda_l$  where  $\lambda_l$  can be significantly larger than  $d$ , implying that a larger amount of conducting material gives rise to more total dissipation, which is entirely sensible. We can also compare the theoretical and experimental normal-state  $R_s$  of Pr-Ce-Cu-O single crystals by using our theoretical expression and by employing the normal state resistivity  $\rho_n \sim 60 \mu\Omega \text{ cm}$  of Pr-Ce-Cu-O and the experimental microwave frequency 9.6 GHz in Ref. 15. We find that theoretically  $R_s(T > T_c) \rightarrow (\mu_0 \omega \rho_n / 2)^{1/2} \sim 0.15 \Omega$  for the Pr-Ce-Cu-O single crystals, which is comparable to the reported surface resistance of  $0.1 \Omega$  within experimental errors. Moreover, as already elaborated in Sec. III, it is reasonable for the electromagnetic dissipation on a very thin conductor with a finite surface area and a small thickness  $d < \delta_n/2$  to be independent of the sample resistance because of incomplete screening. It is also understandable that a very thin conducting film with finite resistivity can yield smaller total microwave absorption than that of a very thick and high-quality superconductor of the same surface area, simply because of the much larger amount of material involved in the latter. Therefore, it is physically accurate that in the dc limit both insulating and conducting thin tapes do yield zero dissipation based on our calculations, because electromagnetic waves cannot propagate through vacuum in the dc limit and therefore no dissipations can occur on thin-film samples separated from the source by vacuum. Finally, we note that in the Comment there appears to be confusion between zero dissipation and perfect conduction in raising some of the objections under this point.

(4) This point criticizes the magnitude of our surface resistance above  $T_c$  by comparing our data with the expression  $R_s = (\rho_n/d)$ , which is not applicable to our samples of small filling factors. We have fully addressed this issue in Sec. III.

(5) The Comment raised the issue that the theoretical fitting curve to our  $R_s(B=0)$  data could not be reproduced with our listed parameter  $(w/a) = 10^{-3}$ . Upon checking the derivations we found the following. In deriving the finite relaxation time  $\tau_0$  of an effective circuit model (see Ref. 16 and Fig. 3) with a junction current density  $J_0$  approximated by the Ambegaokor-Baratoff theory, we had

$$\begin{aligned} \tau_0 &= \frac{\hbar}{2eJ_0a\rho_n} = \left( \frac{\hbar}{2e\rho_n a} \right) \left( \frac{2e\mathcal{R}_n}{\Delta(T)\tanh[\Delta(T)/(2k_B T)]} \right) \\ &= \frac{(\hbar\mathcal{R}_n)/(\rho_n a)}{\Delta(T)\tanh[\Delta(T)/(2k_B T)]}, \end{aligned} \quad (18)$$

where  $\mathcal{R}_n$  is the areal junction resistance,  $a$  is the average grain size of the sample, and  $\Delta(T)$  is the BCS superconducting gap. In theoretical fitting to the zero-field surface resistance, the unknown quantity to be determined by a single fitting parameter was the dimensionless ratio  $C_1 \equiv [\mathcal{R}_n/(\rho_n a)]$ . By taking the expression  $\mathcal{R}_n = (\rho_n w)$  as given in Ref. 2, where  $w$  is the junction width, we obtained a fitting parameter  $C_1 = (w/a) \sim 10^3$ , which would explain the agreement between the data and the fitting curve using  $(w/a) = 1000$  in Fig. 2 of the Comment. This finding therefore indicates that there was a typographic error for the value  $(w/a)$  given in Ref. 2. That is, the parameter should have been  $(w/a) \sim 10^3$  rather than  $10^{-3}$  for the  $B=0$  theoretical curves in Fig. 2 of Ref. 2.

Next we must discuss whether it is reasonable to have  $C_1 \equiv [\mathcal{R}_n/(\rho_n a)] \sim 10^3$ . This consideration requires revisiting the expression for  $\mathcal{R}_n$ . We assumed in Ref. 2 that the areal resistance was given by  $\mathcal{R}_n = (\rho_n w/ad) \times (\text{effective area})$ , where  $(\rho_n w/ad)$  corresponds to the effective resistance of the junction. For  $\mathcal{R}_n = (\rho_n w)$  to be valid, the effective junction area would have to be  $(ad)$ . This seems to be in error, because the junction area should have been  $(wa)$  according to Fig. 3. Thus, we should have had  $C_1 \equiv [\mathcal{R}_n/(\rho_n a)] \sim (w^2/ad) \sim 10^3$  rather than  $C_1 \equiv [\mathcal{R}_n/(\rho_n a)] \sim (w/a) \sim 10^3$ . Noting that the effective junction width ( $w$ ) is comparable to twice the junction penetration depth ( $2\lambda_J$ ) plus the physical thickness of the junction ( $d_J$ ) according to the effective circuit model,<sup>16</sup> we find that the fitting parameter  $C_1 \sim 10^3$  provides the following condition for the grain size  $a$ :

$$\begin{aligned} \frac{w^2}{ad} \sim \frac{(2\lambda_J + d_J)^2}{ad} \sim \frac{2\hbar}{e\mu_0 a^2 d J_c} \sim 10^3, \\ \lambda_J = \left( \frac{\hbar}{2e\mu_0 a J_c} \right)^{1/2}. \end{aligned} \quad (19)$$

Using the empirical values  $d = 130$  nm and  $J_c \sim 5 \times 10^3$  A/m<sup>2</sup>,<sup>17</sup> and assuming that  $d_J \ll \lambda_J$ , we find the grain size  $a \sim 40$   $\mu$ m and  $\lambda_J < 36$   $\mu$ m, which are reasonable. Thus, the relevant question to ask should have been whether  $C_1 \sim (4\lambda_J^2/ad) \sim 10^3 \gg 1$  rather than the condition  $(w/a) \gg 1$  is physically meaningful, and we have shown that the former can be satisfied with realistic physical parameters.

(6) This point criticizes the magnitude, temperature, and frequency dependence of  $R_s$  at  $B=0$ . The criticisms involving the magnitude and temperature dependence of the surface resistance have already been addressed under point 5. On the frequency dependence of the surface resistance, we note that the statement of  $R_s \sim f^\alpha$  with  $\alpha \sim 2$  for  $T \ll T_c$  in Ref. 1 was only meant to be a comment on an approximate experimental observation for the measurements under two

different frequencies. It was not intended to be a theoretical assertion and therefore should not be overinterpreted, because one cannot empirically establish meaningful frequency dependence with only two frequencies. In particular, as described in Sec. II, the WG mode techniques are best for measuring *small relative changes for a given mode as a function of temperature and magnetic field*, but are not ideal for comparing the absolute values of  $R_s$  for samples of significantly different geometries or for measurements under different frequencies, because the antinode positions of different WG modes relative to the sample under these circumstances vary substantially and calibrations must be performed individually for each mode, giving rise to significant inaccuracies in the absolute magnitude. Specifically, if we factor in the uncertainties in the absolute magnitude  $R_s$ , we find that for  $(\delta R_s / \langle R_s \rangle) \approx 20\text{--}30\%$  at  $T \ll T_c$ , where  $\delta R_s$  and  $\langle R_s \rangle$  denote the uncertainty and mean value of  $R_s$ , we obtain

$$\begin{aligned} \frac{R_s(12 \text{ GHz})}{R_s(18 \text{ GHz})} &= \frac{\langle R_s(12 \text{ GHz}) \rangle \pm \delta R_s}{\langle R_s(18 \text{ GHz}) \rangle \pm \delta R_s} \\ &= \frac{\langle R_s(12 \text{ GHz}) \rangle}{\langle R_s(18 \text{ GHz}) \rangle} \left( \frac{1 \pm (\delta R_s / \langle R_s \rangle)_{12 \text{ GHz}}}{1 \pm (\delta R_s / \langle R_s \rangle)_{18 \text{ GHz}}} \right). \end{aligned} \quad (20)$$

If we insert the empirical value of  $\langle R_s(12 \text{ GHz}) \rangle / \langle R_s(18 \text{ GHz}) \rangle \sim 0.4$  and consider maximum errors in accuracy, the ratio of  $R_s$  at 12 GHz relative to that at 18 GHz can vary from  $0.4 \times (0.7/1.3) \sim 0.2$  to  $0.4 \times (1.3/0.7) \sim 0.7$ . We therefore caution against overinterpreting the empirically uncertain frequency dependence.

(7) The Comment criticizes the discrepancy between the empirically determined upper critical field  $B_{c2}(T)$  and the theoretical mean-field  $B_{c2}(T)$  expression. Our understanding is that fluctuation effects are known to play a very significant role in the vortex dynamics of extreme type-II cuprate superconductors. In order to deduce a true second-order vortex phase transition boundary of cuprate superconductors rigorously from experiments, one must make detailed measurements of the relevant physical quantities as a function of temperature near the phase transitions and also as a function of the frequency or currents, and then perform critical scaling analysis of the data near second-order phase transition temperatures. (For more detailed discussions of the strong fluctuation effects and critical scaling analyses of various physical quantities near second-order vortex phase transitions of the cuprates, see, for example, Refs. 4 and 18–22.) On the other hand, it is also well known that the upper critical field  $B_{c2}(T)$  is not a true phase transition for the vortex state of cuprate superconductors, and is better described as a crossover. Hence, there is no rigorous means for us to deduce the upper critical field  $B_{c2}(T)$  from the surface resistance data. Our empirical definition of using the temperatures  $R_s(T, B) = 0.9R_s(T \gg T_c)$  for the  $B_{c2}(T)$  line is only a crude estimate, as we presented in the original discussion of Ref. 1. Furthermore, the high-temperature range under consideration also involves significant thermal fluctuation effects, so that the empirical definition is not expected to be in good agreement with the theoretical mean-field  $B_{c2}(T)$ . On the other hand, at

temperatures sufficiently far away from the phase transitions, the mean-field  $B_{c2}(T)$  formula employed in the Coffey-Clem model is expected to become applicable to the description of vortex dynamics. Thus, there is no real inconsistency between our empirically defined vortex “phase boundary” (or, more precisely, crossover) and the expression for the mean-field upper critical field used in our analyses of vortex dissipation.

(8) The Comment criticizes that we did not use the precise temperature dependence by Coffey and Clem<sup>13,14</sup> or Tinkham<sup>23</sup> in our fitting. For instance, we employed  $[1 - (T/T_c)^2]$  while in Refs. 13 and 14 Coffey and Clem used  $[1 - (T/T_c)^2]/[1 + (T/T_c)^2]$ . In reality, this differentiation is unnecessary particularly near  $T_c$ , because the two expressions only differ by approximately a constant factor over a wide temperature range, which has been absorbed into other zero-temperature fitting parameters  $U_0$ ,  $\lambda_0$ , and  $k_p(0)$ . It is also worth noting that Tinkham’s model for thermally activated phase slippage in an overdamped Josephson junction<sup>23</sup> in 1988 was subsequently widely generalized in the vortex physics community. There have been a vast number of publications on the generalized forms of Tinkham’s model since 1988, and they are often referred to as Tinkham’s model. Several representative literature studies on thermal activation of vortex motion in the cuprates can be found in Refs. 23–27. This is the reason why we referred to the Tinkham and Coffey-Clem models in the context of their key ideas

rather than the exact temperature and field dependence, as long as all relevant information had been explicitly given in our paper.

For heuristic purposes, we show why Tinkham’s model,<sup>23</sup> which was actually extended from a model of Yeshurun and Malozemoff,<sup>24</sup> can come in different forms with varying temperature and magnetic field dependences. If we estimate the activation potential energy  $U$  for pinning of a single vortex, we can approximate  $U$  as the condensation energy density  $(H_c^2/8\pi)$  multiplied by the coherence volume of a vortex, where  $H_c$  is the thermodynamic critical field. In the high-field limit, the coherence volume may be approximated by  $(a_0^2\xi)$ , where  $a_0 \sim (\Phi_0/B)^{1/2}$  is the vortex lattice constant and  $\xi$  the superconducting coherence length. Thus,  $U(T, B) \sim (H_c^2/8\pi)(a_0^2\xi) \sim [1 - (T/T_c)]^{3/2}/B$  in this simple picture, provided that temperature is sufficiently close to  $T_c$  so that  $H_c \sim [1 - (T/T_c)]^{1/2}$  and  $\xi \sim [1 - (T/T_c)]^{-1/2}$ . Subsequent studies revealed the importance of collective vortex pinning effects (see, for example, Refs. 26 and 27). Therefore, the expression for the coherence volume can vary widely if the volume of vortex bundles and the bundle hopping range are considered,<sup>27</sup> so that neither the temperature nor the magnetic field dependence is restricted to the form of  $U(T, B) \sim (H_c^2/8\pi)(a_0^2\xi) \sim [1 - (T/T_c)]^{3/2}/B$  as in the original Tinkham paper.<sup>23</sup>

---

<sup>1</sup>N.-C. Yeh, U. Kriplani, W. Jiang, D. S. Reed, D. M. Strayer, J. B. Barner, B. D. Hunt, M. C. Foote, R. P. Vasquez, A. Gupta, and A. Kussmaul, *Phys. Rev. B* **48**, 9861 (1993).  
<sup>2</sup>N.-C. Yeh, U. Kriplani, W. Jiang, D. S. Reed, D. M. Strayer, A. Gupta, A. Kussmaul, J. B. Barner, B. D. Hunt, M. C. Foote, and R. P. Vasquez, *Phys. Rev. B* **56**, 5683(E) (1997).  
<sup>3</sup>U. Kriplani, N.-C. Yeh, W. Jiang, D. S. Reed, D. M. Strayer, A. Gupta, F. Holtzberg, and A. Kussmaul, in *Layered Superconductors: Fabrication, Properties and Applications*, edited by D. T. Shaw, S. S. Tsuei, T. P. Schneider, and Y. Shiohara, MRS Symposium Proceedings No. 275 (Materials Research Society, Pittsburgh, 1992), pp. 795–800.  
<sup>4</sup>N.-C. Yeh, U. Kriplani, W. Jiang, J. Kumar, H.-F. Fong, D. S. Reed, and C. C. Tsuei, *Int. J. Mod. Phys. B* **11**, 2141 (1997).  
<sup>5</sup>J. D. Jackson, *Classical Electrodynamics*, 2nd ed. (John Wiley & Sons, New York, 1975).  
<sup>6</sup>S. Ramo and J. Whinnery, *Field and Waves in Modern Radio* (Wiley, New York, 1944).  
<sup>7</sup>N. Klein, H. Chaloupka, G. Muller, S. Orbach, H. Peil, B. Roas, L. Schultz, U. Klein, and M. Peiniger, *J. Appl. Phys.* **67**, 6940 (1990).  
<sup>8</sup>M. C. Nuss, P. M. Mankiewich, M. L. O’Malley, E. H. Westerwick, and P. B. Littlewood, *Phys. Rev. Lett.* **66**, 3305 (1991).  
<sup>9</sup>M. C. Nuss, K. W. Goossen, P. M. Mankiewich, and M. L. O’Malley, *Appl. Phys. Lett.* **58**, 2561 (1991).  
<sup>10</sup>Z. Y. Shen, *IEEE Trans. Microwave Theory Tech.* **40**, 2224 (1992).  
<sup>11</sup>C. Wilker, Z. Y. Shen, V. X. Nguyen, and M. S. Brenner, *IEEE Trans. Appl. Supercond.* **3**, 1457 (1993).  
<sup>12</sup>R. J. Ormeno, D. C. Morgan, D. M. Brown, S. F. Lee, and J. R. Waldram, *Rev. Sci. Instrum.* **68**, 2121 (1997).  
<sup>13</sup>M. W. Coffey and J. R. Clem, *Phys. Rev. Lett.* **67**, 386 (1991).  
<sup>14</sup>M. W. Coffey and J. R. Clem, *Phys. Rev. B* **46**, 11757 (1992).  
<sup>15</sup>J. D. Kokales, P. Fournier, L. V. Mercaldo, V. V. Talanov, R. L. Greene, and S. M. Anlage, *Phys. Rev. Lett.* **85**, 3696 (2000).  
<sup>16</sup>T. L. Hylton, A. Kapitulnik, M. R. Beasley, J. P. Carini, L. Drabeck, and G. Gruner, *Appl. Phys. Lett.* **53**, 1345 (1988).  
<sup>17</sup>C. C. Tsuei and J. R. Kirtley, *Phys. Rev. Lett.* **85**, 182 (2000).  
<sup>18</sup>D. S. Reed, N.-C. Yeh, M. Konczykowski, A. V. Samoilov, and F. Holtzberg, *Phys. Rev. B* **51**, 16448 (1995).  
<sup>19</sup>W. Jiang, N.-C. Yeh, D. S. Reed, U. Kriplani, D. A. Beam, M. Konczykowski, T. A. Tombrello, and F. Holtzberg, *Phys. Rev. Lett.* **72**, 550 (1994).  
<sup>20</sup>D. S. Reed, N. C. Yeh, W. Jiang, U. Kriplani, D. A. Beam, and F. Holtzberg, *Phys. Rev. B* **49**, 4384 (1994).  
<sup>21</sup>N.-C. Yeh, D. S. Reed, W. Jiang, U. Kriplani, C. C. Tsuei, C. C. Chi, and F. Holtzberg, *Phys. Rev. Lett.* **71**, 4043 (1993).  
<sup>22</sup>N.-C. Yeh, W. Jiang, D. S. Reed, U. Kriplani, F. Holtzberg, C. C. Tsuei, and C. C. Chi, *Physica A* **200**, 374 (1993).  
<sup>23</sup>M. Tinkham, *Phys. Rev. Lett.* **61**, 1658 (1988).  
<sup>24</sup>Y. Yeshurun and A. P. Malozemoff, *Phys. Rev. Lett.* **60**, 2202 (1988).  
<sup>25</sup>N.-C. Yeh, *Phys. Rev. B* **40**, 4566 (1989).  
<sup>26</sup>P. H. Kes, J. Aarts, J. Vandenberg, C. J. Vanderbeek, and J. A. Mydosh, *Semicond. Sci. Technol.* **1**, 242 (1989).  
<sup>27</sup>For a review of vortex pinning and dynamics in cuprate superconductors, see, for example, G. Blatter, M. V. Feigel’sman, V. B. Geshkenbein, A. I. Larkin, and V. M. Vinokur, *Rev. Mod. Phys.* **66**, 1125 (1994).